# Grazing incidence telescopes: a new class for soft x-ray and EUV spectroscopy

Michael C. Hettrick and Stuart Bowyer

Applied Optics Vol. 23, Issue 21, pp. 3732-3735 (1984)

http://dx.doi.org/10.1364/AO.23.003732



also see addendum at:

Applied Optics Vol. 24, Issue 7, pp. 929-929 (1985)

http://dx.doi.org/10.1364/AO.24.000929

# RAPID COMMUNICATIONS

This section was established to reduce the lead time for the publication of Letters containing new, significant material in rapidly advancing areas of optics judged compelling in their timeliness. The author of such a Letter should have his manuscript reviewed by an OSA Fellow who has similar technical interests and is not a member of the author's institution. The Letter should then be submitted to the Editor, accompanied by a LETTER OF ENDORSEMENT FROM THE OSA FELLOW (who in effect has served as the referee and whose sponsorship will be indicated in the published Letter), A COMMITMENT FROM THE AUTHOR'S INSTITUTION TO PAY THE PUBLICATION CHARGES, and the signed COPYRIGHT TRANSFER AGREEMENT. The Letter will be published without further refereeing. The latest Directory of OSA Members, including Fellows, is published in the July/August 1984 issue of Optics News.

## Grazing incidence telescopes: a new class for soft x-ray and EUV spectroscopy

Michael C. Hettrick and Stuart Bowyer

University of California, Space Sciences Laboratory, Berkeley, California 94720.
Received 16 August 1984.
Sponsored by W. R. Hunter, Naval Research Laboratory.
0003-6935/84/213732-04$02.00/0.


The use of large aperture collecting mirrors is a necessity in astronomy due to the low flux density of incident photons. The optimum properties for such a mirror depend on the instrument it is designed to feed. Historically, at visual wavelengths, optical systems have typically fallen into two categories: (1) telescope/optics systems with wide fields of view for imaging, and (2) telescope/slit spectrometers with narrow fields and slowly diverging beams. These characteristics have usually been obtained with a single telescope followed by relay optics which are changed to optimize the instrument for imaging or spectroscopy. At x-ray wavelengths, where grazing incidence optics are required, imaging systems based on the fundamental analysis by Wolter[1] have been utilized with outstanding success.[2] Similar systems have been developed and used for the extreme ultraviolet[3] (EUV).

The success of these systems combined with the widespread belief that Wolter's analysis was all-encompassing has discouraged further fundamental work in telescope design for x-ray and EUV astronomy. Nonetheless, the use of Wolter systems can lead to cumbersome situations in spectroscopy. For example, the combined length of a Wolter-Schwarzschild type-2 telescope and a slit spectrometer can quickly become prohibitive. Moreover, if such a spectrometer requires a converging beam rather than a diverging beam, additional relay optics must be introduced which lower the throughput. In view of these problems, it would be highly advantageous if a telescope could be designed which specifically optimizes the performance of spectrometers. In this Communication we identify a new such class of grazing incidence telescopes and discuss its advantages for stellar spectroscopy.

The goals we hoped to achieve were (a) the use of a minimum number of reflecting surfaces to permit high throughput, (b) the use of an aperture stop (or large pinhole) to reduce background contamination, (c) the ability to obtain a desired beam $f$/No. within a minimum overall length to reduce satellite costs, and (d) a reasonable working field to allow onboard spacecraft tracking, field star verification of targets, and to retain a capability for long-slit spectroscopy on extended sources.

The requirement of an imaging field requires two or a larger even number of reflecting surfaces. A fundamental point, however, and the key to the proposed design is that both reflections need not occur before the aperture stop. In stellar spectroscopy, the image quality at this stop need only be sufficient to reduce background contamination and to prevent confusion from nearby stars. With the additional constraints of a minimum overall length and a minimum number of reflections, we anticipate the ideal optical system to be one which consists of two surfaces of revolution between which exists a primary focus and an aperture stop. In Fig. 1 we illustrate such a class of geometric solutions. Figure 1(a) shows a type I, which provides a converging beam at the exit of the telescope. In simplest form, the mirror surfaces are conic sections of revolution:

$$z_1 = s + \tfrac{1}{2}r_1^2/r_{1\max}/\tan(\gamma_{1\min}) - \tfrac{1}{2}r_{1\max}\tan(\gamma_{1\min}), \quad (1)$$

$$z_2 = s/2 + a\sqrt{1-(r_2/b)^2}. \quad (2)$$

These are equations of a paraboloid and a confocal ellipsoid. The coordinates $z_1$ and $z_2$ are the primary and secondary

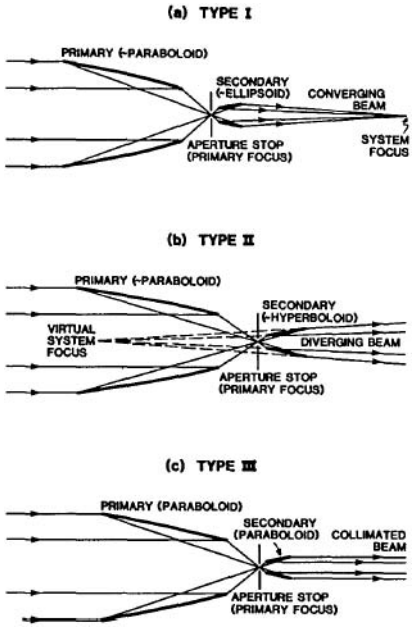


Fig. 1. Proposed telescope geometry consisting of a primary and a secondary both at grazing incidence: (a) type I delivers a converging beam having a real focus, (b) type II delivers a diverging beam from a virtual focus, (c) type III delivers a collimated beam concentrated relative to the primary aperture. Diffuse background is largely removed by a pinhole placed at the primary mirror focus. For most applications, conic sections (paraboloids, ellipsoids, and hyperboloids) can be used, however deformed surfaces exhibiting coma-free fields can also be used.

projections on the optical axis and are measured from the system focus; $r_1$ and $r_2$ are the radial coordinates from this axis. The parameter $s$ is the separation between the primary and system foci, and $a$ and $b$ are the semiminor and semimajor axes of the elliptical secondary. In terms of convenient input parameters, we have

$$s = z_{1\max} - r_{1\max}/\tan(2\gamma_{1\min}), \tag{3}$$

$$(a/s)^2 = (\eta - 1)/(\eta + 1)^2[\tfrac{1}{4}(\eta - 1) + \tfrac{1}{2}\eta \tan(\alpha_{\max})/\tan(\gamma_{1\min} - \alpha_{\max}/2)], \tag{4}$$

$$(b/s)^2 = \eta \tan(\alpha_{\max})/(\eta + 1)^2[\eta \tan(\alpha_{\max}) + \tfrac{1}{2}(\eta - 1)\tan(\gamma_{1\min} - \alpha_{\max}/2)], \tag{5}$$

where

$$\alpha_{\max} = \arcsin(r_{1\max}/f), \tag{6}$$

$$\eta \equiv \tan(2\gamma_{1\min})/\tan(\alpha_{\max}). \tag{7}$$

There are five input parameters: $r_{1\min}$,$r_{1\max}$,$z_{1\max}$, the effective focal length $f$, and the minimum graze angle $\gamma_{1\min}$ for axial rays on the primary. The resulting maximum and minimum radii of the secondary mirror are

$$r_{2\max} = s\eta/(\eta + 1)\tan(\alpha_{\max}), \tag{8}$$

$$r_{2\min}(z_{1\min} - s) = r_{1\min}(s - z_{2\max}). \tag{9}$$

where $z_{2\max} = z_2$ at $r_{2\min}$. Equations (9) and (2) yield a quadratic equation whose positive root is the solution for $r_{2\min}$. The value for $\alpha_{\min}$ is then determined: $\alpha_{\min} = \arctan(r_{2\min}/z_{2\max})$. The cone angles $\alpha$ do not therefore follow the Abbe sine rule,[1,4] although the numerical deviations are calculated to be very small. It is noted that Eq. (6) defines the focal length $f$ rather than representing the sine rule.

The results of ray trace calculations, shown in Fig. 2, reveal that this two-element mirror system provides excellent off-axis imaging at the system focus. The telescope is defined by an $f10$ beam, a primary mirror filling an aperture from 0.5 to 1.0 m in diameter, a front-focus axial length $z_{1\max} = 4.5$ m, and a minimum graze angle $\gamma_{1\min} = 7.2°$. We have placed a flat detector at the Gaussian focus and have plotted the root-mean-square (rms) spot radius as a function of the off-axis field angle. The straight line which is fitted to the computed values has a slope of two on this log–log plot. No coma (slope = 1) was present in these calculations, even for spots as small as $10^{-3}$ sec of arc. This indicates that any offense against the sine rule is small. In particular, it should be noted that a blur radius of 0.5 sec of arc rms is obtained at 1 min of arc off-axis. Such performance is more than adequate for use as a collecting mirror which feeds a high resolution spectrometer. Vignetting is found to be 10% at 30 min of arc off-axis if the secondary mirror is not extended (only long enough to intercept 100% of the on-axis rays). At the primary mirror focus, the spot radius is found to equal the off-axis field angle, which is precisely the pinhole radius required to ensure acquisition of the target. Thus, the use of a paraboloid does not require a larger pinhole.

For comparison, ray trace results are also shown in Fig. 2 for a Wolter-Schwarzschild (W-S) type-2 telescope which fits within the same physical envelope and has equal throughput but cannot feature an aperture stop at the primary focus. Our new type-I design shows aberrations which are only a factor of 2 larger than the W-S type-2. In another example, using $f3$ beams, the type-I aberrations were a factor of 3.5 larger. For both the W-S type-2 and the new telescope, an optimally curved detector was found to reduce field aberrations by an order of magnitude, however the required radius of curvature is impractically small (<1 cm). Figure 2, also shows results

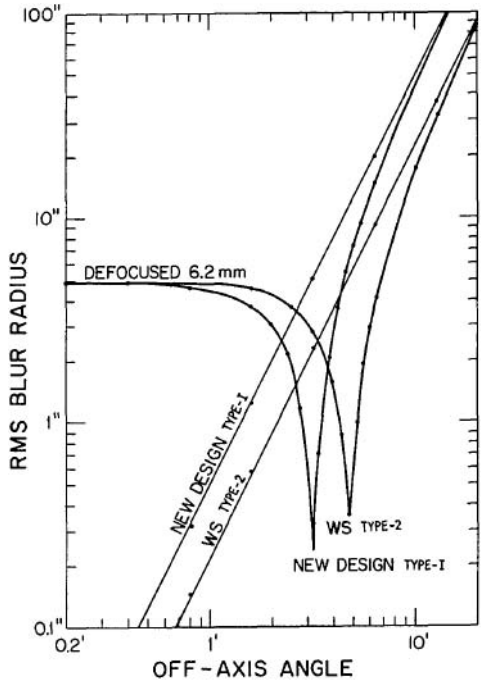


Fig. 2. Ray traces for the proposed grazing incidence two-element paraboloid–ellipsoid telescope (type I) compared with a Wolter-Schwarzschild type-2 system. 500 rays were placed randomly within the aperture of the primary mirror described in the text. The dots represent the calculated rms image radius at several off-axis angles. Ray traces of the deformed surfaces with Schwarzschild parameters $\rho_0 = -f/3.9$ and $\Delta = -f/251.64$ are indistinguishable to those of the conic sections. Ray traces were performed using flat detectors situated at the Gaussian on-axis focus (straight lines) and displaced from this plane by 6.2 mm (curves).

using flat detectors displaced from the Gaussian focus by 0.62 cm. This results in a significant reduction of aberrations only within a narrow range of off-axis angles and results in significant defocusing of the on-axis image.

We examined the possibility that the proposed mirror system was embedded within Schwarzschild's equations for coma-free telescope systems of revolution[4]:

$$z_1 = \Delta - (f^2/4\Delta)\sin^2\alpha - \rho_0[1 - (f/\Delta)\sin^2(\alpha/2)]^{\frac{2\Delta - f}{\Delta - f}}[\cos^2(\alpha/2)]^{-\frac{f}{\Delta - f}}, \tag{10}$$

$$r_1 = f\sin\alpha, \tag{11}$$

$$z_2 = -\rho\cos\alpha, \tag{12}$$

$$r_2 = \rho\sin\alpha, \tag{13}$$

where

$$1/\rho = (1/\Delta)\sin^2(\alpha/2) + (1/\rho_0)[1 - (f/\Delta)\sin^2(\alpha/2)]^{-\frac{f}{\Delta - f}}[\cos^2(\alpha/2)]^{\frac{\Delta}{\Delta - f}}. \tag{14}$$

In these parametric equations, $f$ is the effective focal length, and $z_1$, $z_2$, $r_1$, and $r_2$ are the axial and radial coordinates of the primary and secondary mirror surfaces. The parameter $\alpha$ equals the cone angle made by the exiting ray relative to the optical axis, as defined previously. Since these equations generate mirror systems which are strictly free of coma, $\alpha$ is obtained from the Abbe sine rule[1,4]: $\alpha = \arcsin(r_1/f)$. The quantities $\Delta$ and $\rho_0$ are integration constants which set the

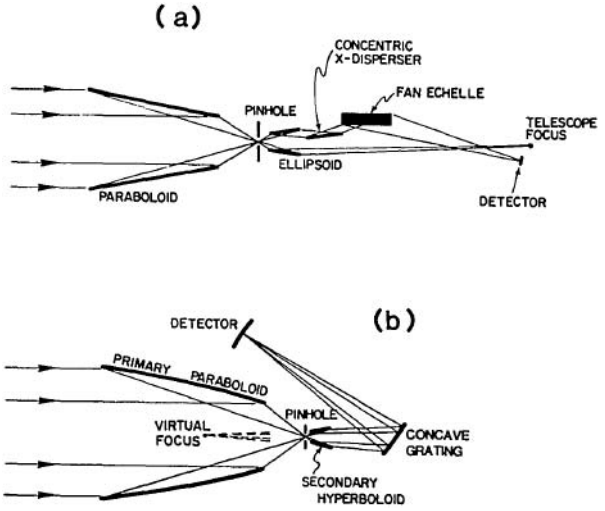


Fig. 3.(a) Grazing incidence telescope–spectrometer instrument consisting of only four grazing reflections. The echelle is a conical diffraction fan grating, and the cross disperser is a concentric groove grating, both as described in Refs. 5 and 6. Shown is one of the four identical grating systems which can be inserted into the converging beam. Diffuse background is largely removed by a pinhole placed at the primary mirror focus. (b) Normal incidence Rowland circle spectrometer fed by the diverging beam from a type-II new-class grazing incidence telescope. Diffuse background is largely removed by a pinhole placed at the primary mirror focus.

particular surface functions. Geometrically, $\rho_0$ is the distance between the focus and the secondary vertex and $\rho_0 - \Delta$ is the distance between the focus and the primary vertex. Wolter[1] has described grazing incidence systems of type 1, type 2, and type 3 which result from use of Eqs. (10)–(14) with various choices for $\Delta$ and $\rho_0$. The Wolter-Schwarzschild type-1 systems result from use of a positive real value for $\Delta$ and a complex value for $\rho_0$; type 2 and type 3 result from use of positive real values for both $\Delta$ and $\rho_0$. However, none of these contains a primary mirror focus prior to the secondary. In contrast, we found that our proposed type-I system results from use of negative real numbers for $\Delta$ ($<0$) and $\rho_0$ ($\ll 0$). In this case, Eqs. (10)–(14) represent deformed paraboloid–ellipsoid mirrors which are strictly coma-free and contain a focus between the two elements. Ray traces of these deformed surfaces yielded results indistinguishable from those obtained previously in Fig. 2 for the paraboloid–ellipsoid, verifying that coma is not dominant in the latter case.

In permitting negative values for the Schwarzschild parameters in Eqs. (10)–(14), other new families of grazing incidence telescope solutions can be obtained. For example, if $\Delta > 0$ and $\rho_0 \ll 0$, we found that the exiting beam diverges from a virtual focus, following convergence to a primary focus. The two mirror surfaces are approximately a paraboloid and hyperboloid, as shown in Fig. 1(b). Such a telescope, which like the type I contains a primary focus in advance of the secondary, we classify as a type II. In the extreme case as $f \to \infty$, $\alpha \to 0$, and $\rho_0 \to -\infty$, Schwarzschild's equations degenerate into the confocal paraboloids:

$$z_1 = \Delta - r_1^2/4\Delta, \tag{15}$$

$$z_2 = \Delta/c - r_2^2/(4\Delta/c), \tag{16}$$

where $c \equiv f/\rho_0 < 0$ and $\Delta < 0$. This type-III system, illustrated in Fig. 1(c), produces a collimated beam which is concentrated by the factor $|c|$ relative to the primary aperture. In Eqs. (15) and (16), $z = 0$ is located at the confocal point (the primary focus).

Telescope types I, II, and III as described above constitute a new design class distinguished from others at grazing incidence by the presence of a primary real focus between the two mirror elements. It is interesting to note, using Eqs. (10)–(14), that, if $\Delta$ and $\rho_0$ are both negative, small ($\sim 2$), and comparable, a classical Gregorian normal incidence telescope is obtained.

The telescope designs proposed above were motivated by their spectroscopic applications. For example, type I delivers a converging beam preceded by a pinhole. This geometry is ideal for feeding spectrometer designs employing variable line-space plane gratings which have been shown to exhibit anomalously high performance at grazing incidence.[5,6] A two-grating design (concentric groove grating plus oriental fan grating) can produce an echellogram on a 2-D imaging detector. In Fig. 3(a) we show one of four such grating systems which combined fill the converging beam behind a type-I telescope. Note that this instrument is very short due to the aperture stop being located significantly in advance of the system focus.

To estimate some of the performance characteristics of such a telescope/spectrograph instrument, we used the 1-m diam telescope whose ray trace was presented in Fig. 2. Figure 4 plots the effective area for the instrument shown in Fig. 3(a). The geometric collecting area of the telescope is 5890 cm$^2$. Platinum surfaces are assumed throughout, with reflectivities obtained from the optical data of Ref. 7. The dark curve indicates the effective area for the telescope, while the light curves plot the effective area for the complete spectrographic instrument. This includes a detector with 30% quantum efficiency and gratings at graze angles of 8° and 15°. The net efficiency of the telescope plus spectrograph is calculated to be 2.5–5.5% (with the detector efficiency this becomes 0.8–1.7%). This high efficiency delivers ~80 cm$^2$ of effective area in the 900–1200-Å band and 50–100 cm$^2$ in the EUV. These

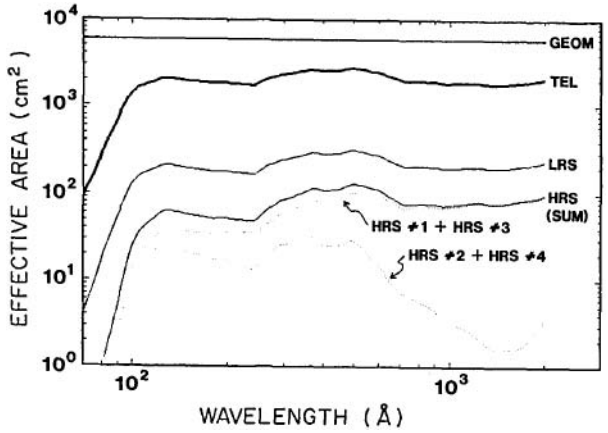


Fig. 4. Effective collecting area for the grazing spectrometer of Fig. 3(a), including reflection efficiency of the telescope and gratings, diffraction efficiency of the gratings, and quantum efficiency of the detector. All wavelengths are assumed to be at the blaze of the cross disperser. In the 900–1200-Å region an effective area of 80 cm$^2$ is obtained with high resolution (HRS) echelle systems. If the incident light is 100% linearly polarized, the dotted curves show separately the efficiency of grating systems #1 + #3 and orthogonally situated grating systems #2 + #4. A lower dispersion system (LRS) in which the echelle grating is removed attains 200 cm$^2$ in the extreme and far ultraviolet.

estimates assume the wavelength of interest is blazed by the cross disperser. If the four plane grating systems are mounted at right angles to each other, the polarization dependence of reflection coefficients results in spectropolarimetry at wavelengths longward of ~200 Å (dotted curves in Fig. 4). If the echelle is removed, a lower resolution instrument is obtained with an effective area of 150–300 $cm^2$ in the 100–2000-Å wavelength range.

This instrument also exhibits excellent background rejection capabilities. The axial distance from the primary entrance aperture to the aperture stop is 174 cm. Assuming the telescope points with an accuracy of ±4 sec of arc relative to a stellar source, this stop can be as small as 68 $\mu$m in diameter and will therefore be referred to as a pinhole. This pinhole subtends a sky solid angle of only $\sim 10^{-9}$ sr, with the result that very intense diffuse backgrounds are rejected. For example, even the dominant hydrogen $L_\alpha$(1216 Å) geocoronal line (3000 rayleighs) would contribute only 20 counts/sec, integrated over the directly contaminated region of the spectrum near $\lambda$ = 1216 Å. Using 0.5 × 10 sec of arc resolution elements, this converts to only 0.25 counts/sec in each bin near 1216 Å. Furthermore, the pinhole removes such direct contamination away from the immediate spectral vicinity of $L_\alpha$. For example, at $\lambda/\Delta\lambda$ = 30,000, background is removed at all wavelengths at least 0.3 Å away from 1215.7 Å. Imperfections in the grating(s) will also give rise to low levels of indirect scattered light, which for echelles operating at these wavelengths are typically $10^{-2}$/Å times the integrated direct intensity.[8] With bins of 0.03 Å and with direct intensities of the order of 20 counts/sec, this contributes only a few × $10^{-3}$ counts/sec/bin.

Another spectrograph which is substantially improved by use of the proposed class of telescopes is the conventional normal incidence Rowland circle grating. The type-II telescope delivers the required diverging beam but one which diverges from a virtual focus. This permits an extremely compact spectrometer in which the diffracted beam is folded back to the primary aperture of the telescope. Such an instrument is illustrated in Fig. 3(b). It is instructive to compare this instrument with other related approaches. Compared with the use of a conventional Wolter type-2 telescope whose only focus is located downstream of the secondary mirror, the length of a normal incidence Rowland circle instrument is reduced by the length of the spectrometer plus a major portion of the secondary-to-focus distance of the telescope. In another approach, Chase *et al.*[9] studied systematically the properties of relay optics at grazing incidence and have considered feeding spectrographs through such optics which modify the beam of Wolter type-1 x-ray telescopes. Both one-element and two-element relay optics were considered, the latter being necessary if an imaging field is required. Using a new-design imaging telescope (e.g., type II feeding a Rowland circle), there are two less reflections, with the result that throughput is significantly increased. However, the four-element systems permit imaging of extended sources at the telescope focus and thus long-slit spectroscopy.

To summarize: we have proposed a new class of grazing incidence telescopes. Schwarzschild's equations for coma-free imaging systems can be extended to include this geometry by allowing negative values for the integration constants. However, for the examples ray traced (type I), deformed surfaces exhibited no substantial improvements in imaging over simple conic sections. The three telescope types possess unique properties which improve the efficiency and shorten the lengths of soft x-ray/EUV spectrographs. In future papers we intend to explore in detail the properties of such designs and to develop solutions optimized for particular applications.

*Note added in proof:* The phrase "aperture stop", as used in the text and in figure 1, should be replaced by the phrase "field stop". The authors thank P. Davila for suggesting this more appropriate terminology.

We thank Pat Jelinsky, James Green, and Michael Lampton for helpful discussions. This work was supported by NASA grant NAG 5-420.

Stuart Bowyer also holds an appointment with the University of California, Astronomy Department, Berkeley.

## References

1. H. Wolter, "Spiegelsysteme streifenden Einfalls als abbildende Optiken für Röntgenstrahlen," Ann. Phys. **10,** 94, 286 (1952).
2. R. Giacconi *et al.*, "The Einstein (HEAO 2) X-Ray Observatory," Astrophys. J. **230,** 540 (1979).
3. R. F. Malina, S. Bowyer, D. Finley, and W. Cash, "Wolter-Schwarzschild Optics for the Extreme Ultraviolet: the Berkeley Spectrometer and the EUV Explorer," Opt. Eng. **19,** 211 (1980).
4. J. Picht, "Bestimmung eines aus einem (beliebigen) Paraboloid-spiegel und einem Zwei-Spiegel-Zusatzsystem bestehenden Drei-Spiegel-Systems, für das die Aufhebung der sphärischen Aberration sowie die Sinusbedingung (Komafreiheit) streng erfüllt ist. Untersuchungen über den Ersatz jener (deformierten) Hilfs-spiegel durch einfacher herstellbare Spiegelflächen," Optik **8,** 129 (1951); K. Schwarzschild, "Untersuchungen zur geometrischen Optik. II. Theorie der Spiegeltelescope," Abh. Akad. Wiss. Goettingen, **4,** No. 2, 1 (1905).
5. M. C. Hettrick and S. Bowyer, "Variable Line-Space Gratings: New Designs for Use in Grazing Incidence Spectrometers," Appl. Opt. **22,** 3921 (1983).
6. M. C. Hettrick, "Aberrations of Variable Line-Space Grazing Incidence Gratings in Converging Light Beams," Appl. Opt. **23,** 3221 (1984).
7. W. R. Hunter, D. W. Angel, and G. Hass, "Optical Properties of Evaporated Platinum Films in the Vacuum Ultraviolet from 2200 Å to 150 Å," J. Opt. Soc. Am. **69,** 1695 (1979).
8. G. H. Mount and W. G. Fastie, "Comprehensive Analysis of Gratings for Ultraviolet Space Instrumentation," Appl. Opt. **17,** 3108 (1978).
9. R. C. Chase, A. S. Krieger, and J. H. Underwood, "Grazing Incidence Relay Optics," Appl. Opt. **21,** 4446 (1982).